RI 9162

Bureau of Mines Report of Investigations/1988

Roof Truss Contact Forces

By J. H. Stears and M. O. Serbousek

UNITED STATES DEPARTMENT OF THE INTERIOR

Report of Investigations 9162

Roof Truss Contact Forces

By J. H. Stears and M. O. Serbousek

UNITED STATES DEPARTMENT OF THE INTERIOR
Donald Paul Hodel, Secretary

BUREAU OF MINES
T S Ary, Director

Library of Congress Cataloging in Publication Data:

Stears, J. H. (Juel H.)
Roof truss contact forces.

(Bureau of Mines report of investigations ; 9162)

Supt. of Docs. no.: I 28.23:9162.

1. Mine roof control. 2. Roof trusses. I. Serbousek, M. O. (Maynard O.) II. Title. III. Series: Report of investigations (United States. Bureau of Mines) ; 9162.

TN23.U43 [TN288] 622 s [622'.28] 88-600004

CONTENTS

ILLUSTRATIONS

TABLES

UNIT OF MEASURE ABBREVIATIONS USED IN THIS REPORT

deg	degree	pct	percent
ft	foot	psi	pound (force) per square inch
in	inch	yr	year
lb	pound		

ROOF TRUSS CONTACT FORCES

By J. H. Stears[1] and M. O. Serbousek[2]

ABSTRACT

Increasing use of Birmingham and other roof trusses prompted a Bureau of Mines study of support forces produced on a mine roof by these members. Equations, obtained from laboratory and field tests, are given for calculating the contact forces between the roof strata and a typical truss. Actual contact forces for a specific truss are difficult to estimate because of variable friction loss at the contact points. A finite-element analysis, using typical contact forces, indicated that trusses have a negligible effect on the stress field in massive, competent roof strata. The effectiveness of trusses in supporting broken rock strata was not analyzed. However, experience has shown that trusses are effective in supporting incompetent roof.

[1]Mining engineer.
[2]Structural engineer.
Spokane Research Center, Bureau of Mines, Spokane, WA.

INTRODUCTION

Mine Safety and Health Administration accident statistics show that roof falls have always been a major cause of underground accidents and fatalities. Although roof bolts are normally used for coal mine roof support, in some areas with poor roof conditions, roof trusses provide better roof support than roof bolts.

The mechanism by which trusses contribute to roof stability is poorly understood. Since Claude White introduced the Brimingham truss[3] in 1967, numerous articles have been published on roof trusses. Among these is a report[4] by the faculty of Virginia Polytechnic Institute describing a combined photoelastic, finite-element study of roof stresses and deflections. In another article, Mangelsdorf[5] studied the tension variations in different segments of the Birmingham roof truss caused by friction at the contact points between the truss and the roof.

Tensioned roof bolts provide an uplifting force on the roof strata at the bolthead and these forces help to hold the roof rock in place. One aspect of the problem concerns the magnitude of component forces applied to roof strata by the truss and the effect of these forces on roof behavior. The objective of the present study was to measure the vertical and horizontal components of those reaction forces between a Birmingham truss and an instrumented test frame used for various truss configurations. These forces were then entered into an elastic finite-element analysis to estimate their effects upon strata stresses and deflections.

BIRMINGHAM TRUSS

The roof truss as developed by the Birmingham Bolt Co. is shown in figure 1. It consists of two inclined chords anchored in drill holes and one horizontal chord running below the roof surface. The drill holes are usually inclined at 45° angles and are deep enough so that the anchors are placed in unbroken strata over the ribs. Either a mechanical or resin anchor can be used. Recent tests[6] indicate that a 2-ft-long resin anchor gives adequate holding power. Truss rods are usually made from 11/16-in-diameter steel rod with 3/4-in rolled threads. The length of the truss assembly can be adjusted by the operator to vary the different distances between hole collars.

The truss is tensioned either by rotating the turnbuckle or by hydraulic tensioning of a flanged nut. A steel bearing plate is used on each side of the truss to distribute the force applied to the roof over a larger surface area. The truss rod normally contacts the roof directly at the hole collar and indirectly through the bearing plate. The manufacturer claims that tensioning the truss creates an upward thrust upon the roof rock and generates compressive forces in the lower roof strata.

---

[3]Reference to specific products does not imply endorsement by the Bureau of Mines.

[4]Department of Mining and Minerals Engineering, Virginia Polytechnic Institute. Design Optimization in Underground Coal Systems, Volume VIII, The Roof Truss: An Analysis With Applications to Mine Design. Final Tech. Rep. to U.S. Dep. of Energy, 1981, 341 pp.

[5]Mangelsdorf, C. P. Evaluation of Roof Trusses, Phase I (grant G0166088, Univ. Pittsburgh). BuMines OFR 56-82, 1979, 111 pp., NTIS PB 82-209768.

[6]Mallicoat, W. R. Truss Bolting With Point Resin Anchorage. Min. Congr. J., June 1978, pp. 47-50.

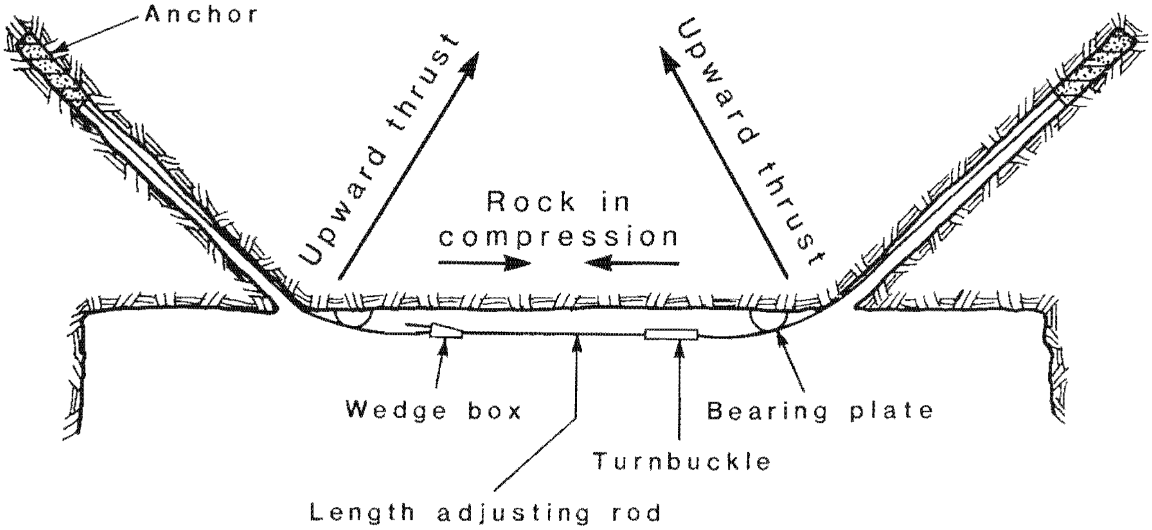

FIGURE 1.—Birmingham roof truss.

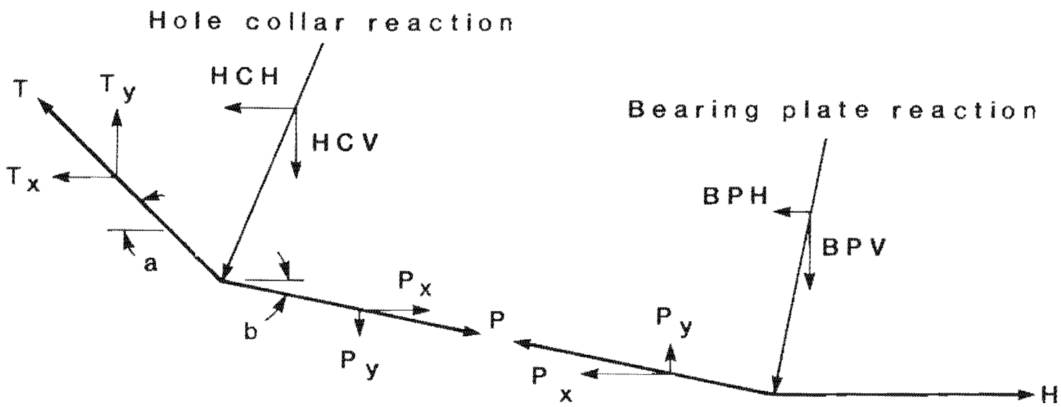

FIGURE 2.—Free-body diagram of truss system.

EQUILIBRIUM EQUATIONS

A free-body diagram of one side of a truss is shown in figure 2. T is the tension in the inclined rod going to the anchor, H is the tension in the horizontal rod going to the turnbuckle, and P is the tension in the rod segment between the hole collar and the bearing plate. The inclinations from the horizontal of T and P are given by a and b. If the roof line is flat and level, then the tangent of b would equal the height of the bearing plate divided by its distance from the hole collar. The horizontal and vertical components of the forces are denoted on the figure as P_x, P_y,...., P_n. From trigonometric relations:

$$P_y = P \sin b, \tag{1}$$

$$P_x = P \cos b, \tag{2}$$

$$T_y = T \sin a, \tag{3}$$

and

$$T_x = T \cos a. \tag{4}$$

Reaction forces occur where the truss rod touches the roof at the hole collar and the bearing plate. The vertical component of the bearing plate reaction is denoted as bearing plate vertical (BPV), while the horizontal component is denoted as bearing plate horizontal (BPH). The reaction components at the hole collar are similarly designated as hole collar vertical (HCV) and hole collar horizontal (HCH). Summing forces in the vertical and horizontal directions at the bearing plate results in the equations:

$$BPV = P_y = P \sin b \tag{5}$$

and

$$BPH = H - P_x = H - P \cos b. \tag{6}$$

Summing forces in the vertical and horizontal directions at the hole collar results in

$$HCV = T_y - P_y = T \sin a - P \sin b \tag{7}$$

and

$$HCH = P_x - T_x = P \cos b - T \cos a. \tag{8}$$

Equations 5 through 8 are the equilibrium equations expressing the relationships between the truss rod tensions and the reaction forces.

As the turnbuckle is rotated, it pulls the threaded end of the truss rod into itself, which moves the truss rod across the contact points at the hole collar and bearing plate, and generates a friction force at these contact points. Consequently, T will be smaller than P and P will be smaller than H because of frictional force losses at the contact points. As these frictional forces are internal to the free-body diagram of figure 2, they are not included in the equilibrium equations. Their effects will show up in the changing values of P and T due to friction loss, which will, in turn, change the magnitude of the reaction components according to the equilibrium equations.

The equilibrium equations can be put into dimensionless form by dividing each term by H. Therefore,

$$\frac{BPV}{H} = \frac{P}{H} \sin b, \tag{9}$$

$$\frac{BPH}{H} = 1 - \frac{P}{H} \cos b, \tag{10}$$

$$\frac{HCV}{H} = \frac{T}{H} \sin a - \frac{P}{H} \sin b, \tag{11}$$

and

$$\frac{HCH}{H} = \frac{P}{H} \cos b - \frac{T}{H} \cos a. \tag{12}$$

Theoretical curves of BPV-H are shown in figure 3. The abscissa is marked both with the sine of b and the corresponding distances from the hole collar for a 2-in-high bearing plate. The curves show

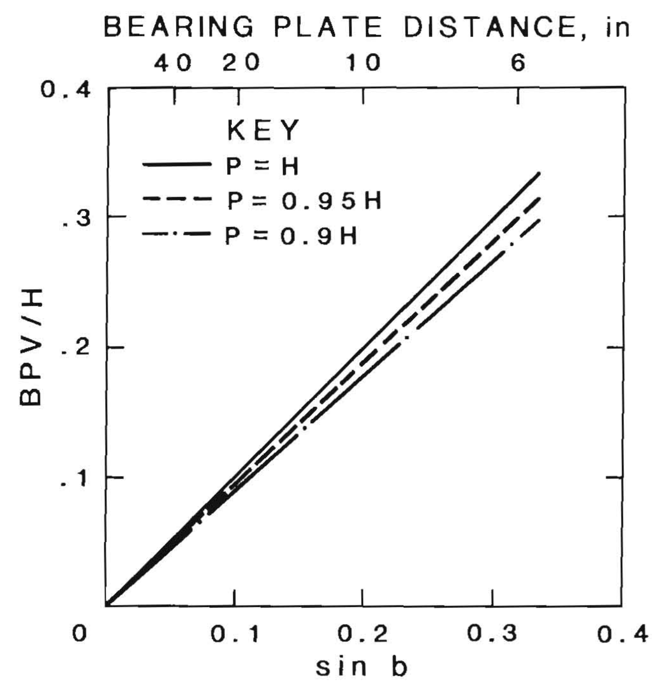

FIGURE 3.—Theoretical curves of vertical reaction component at the bearing plate.

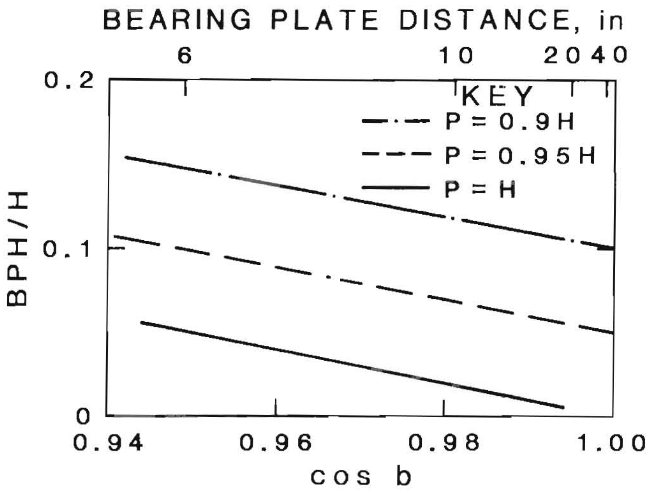

FIGURE 4.—Theoretical curves of horizontal reaction component at the bearing plate.

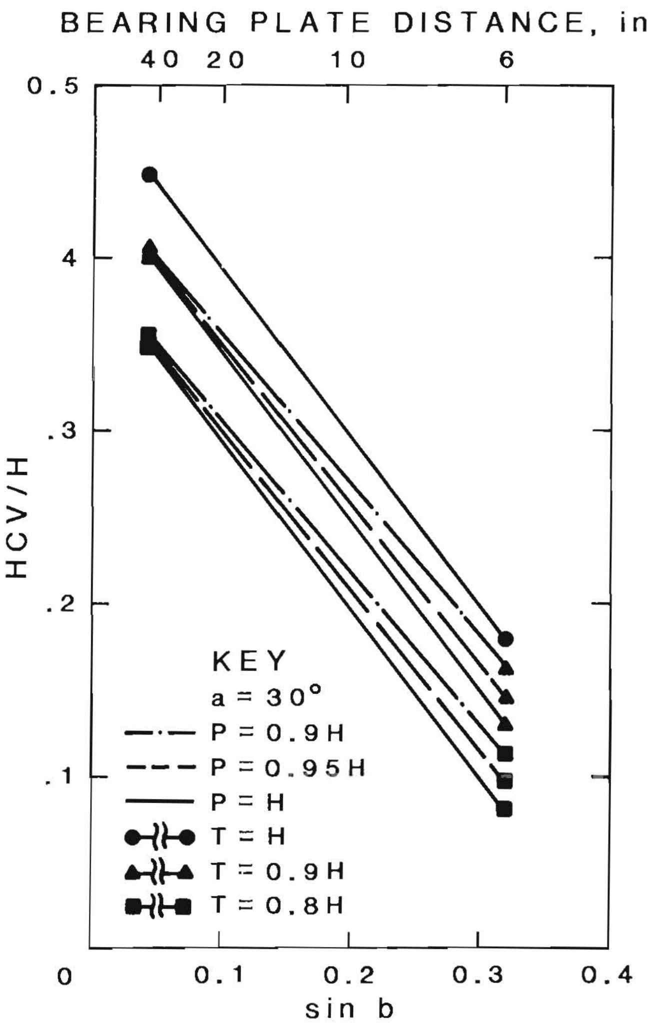

FIGURE 5.—Theoretical curves of vertical reaction component at hole collar for a = 30°.

that the vertical component of the bearing plate reaction increases as the bearing plate gets closer to the hole collar, and that it increases as the P-H ratio becomes closer to 1, i.e., P = H.

Theoretical curves of BPH-H are shown in figure 4. The horizontal component of the bearing plate reaction is greatest when the bearing plate is close to the hole collar and the P-H ratio is less than 1.

It is difficult to show the hole collar reaction components on one graph as they depend on four variables. Theoretical curves of HCV-H for a equal to 30°, 45°, and 60° are shown in figures 5, 6, and 7, respectively. In general, the curves indicate that the vertical component is greatest when the bearing plate is farthest from the hole collar, the T-H ratio is close to 1, and the P-H ratio is less than 1.

Theoretical curves of HCH-H for the three angles of a are shown in figures 8, 9 and 10. The curves show that the horizontal component is greatest when the bearing plate is farthest from the hole collar, the T-H ratio is less than 1, and the P-H ratio is close to 1.

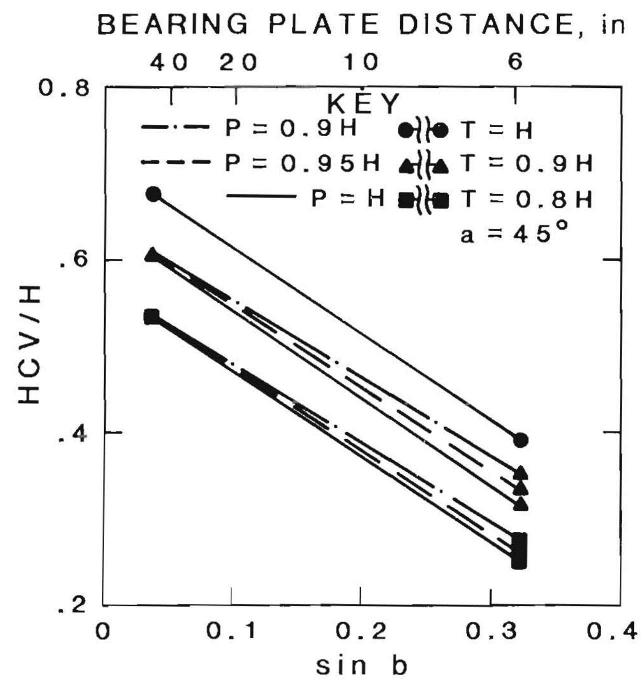

FIGURE 6.—Theoretical curves of vertical reaction component at hole collar for a = 45°.

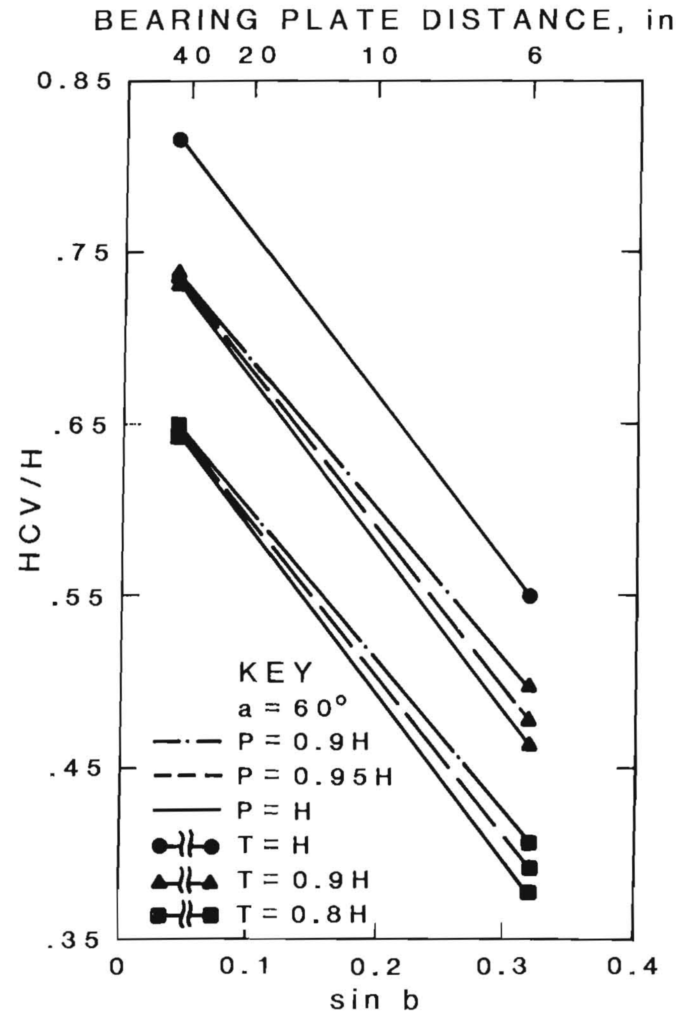

FIGURE 7.—Theoretical curves of vertical reaction component at hole collar for a = 60°.

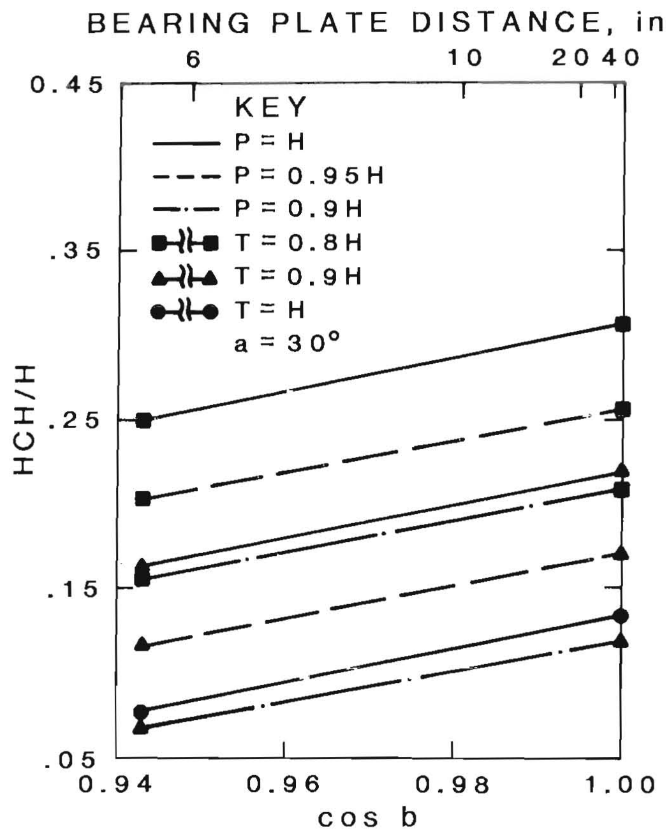

FIGURE 8.—Theoretical curves of horizontal reaction component at hole collar for a = 30°.

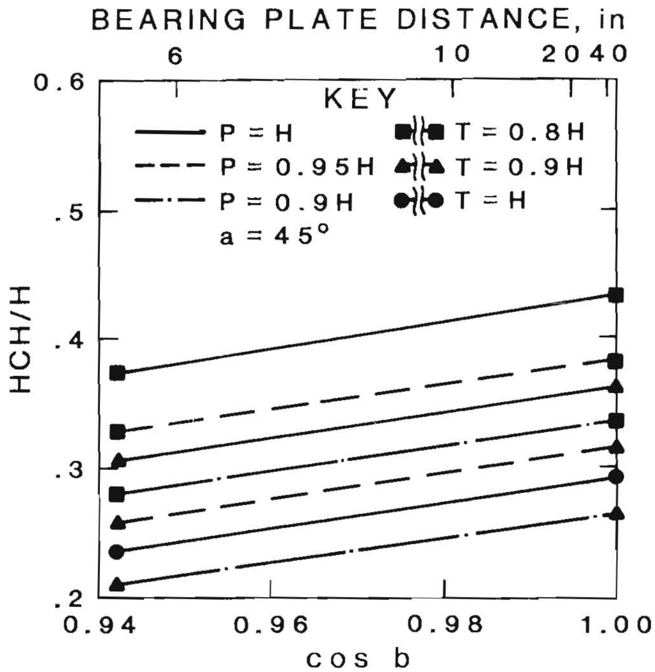

FIGURE 9.—Theoretical curves of horizontal reaction component at hole collar for a = 45°.

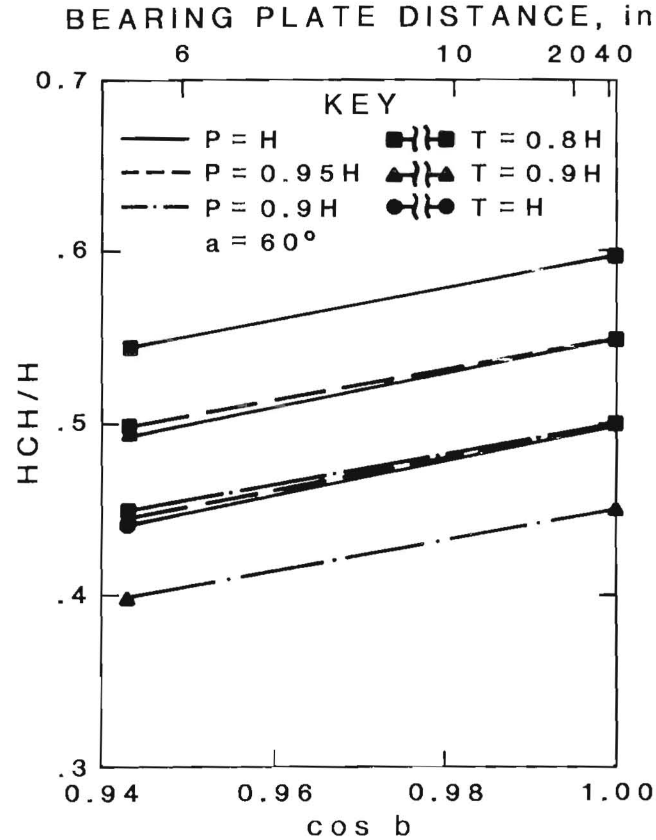

FIGURE 10.—Theoretical curves of horizontal reaction component at hole collar for a = 60°.

EXPERIMENTAL EQUIPMENT

TRUSS TESTING FRAME

A drawing of the truss testing frame is shown in figure 11. The top and bottom frame members were made of 8-in-square steel tubing with the bottom bolted to the reinforced concrete test floor. The vertical members were made of C 10x30 channels, positioned on both sides of the tubing, and bolted to the tubing with 1-in-diameter structural steel bolts. Overall dimensions were 14 ft high by 16 ft long. A truss support beam, also made of 8-in-square tubing, was positioned at the various heights needed for the different inclined chord angles. The truss was placed on top of the truss support beam and connected to the floor anchors.

LOAD CELLS

Four different types of load cells were used to measure the experimental forces.

Turnbuckle

Strain gauges were mounted on a standard Birmingham truss turnbuckle to measure the tension in the horizontal leg of the truss. The outer surface of the turnbuckle was machined lightly to remove rust and scale. Two 350-ohm, foil-type gauges were mounted 180° apart about 2-1/4 in from the end of the turnbuckle and wired into opposite arms of a Wheatstone bridge. Two compensating gauges were used to complete the bridge

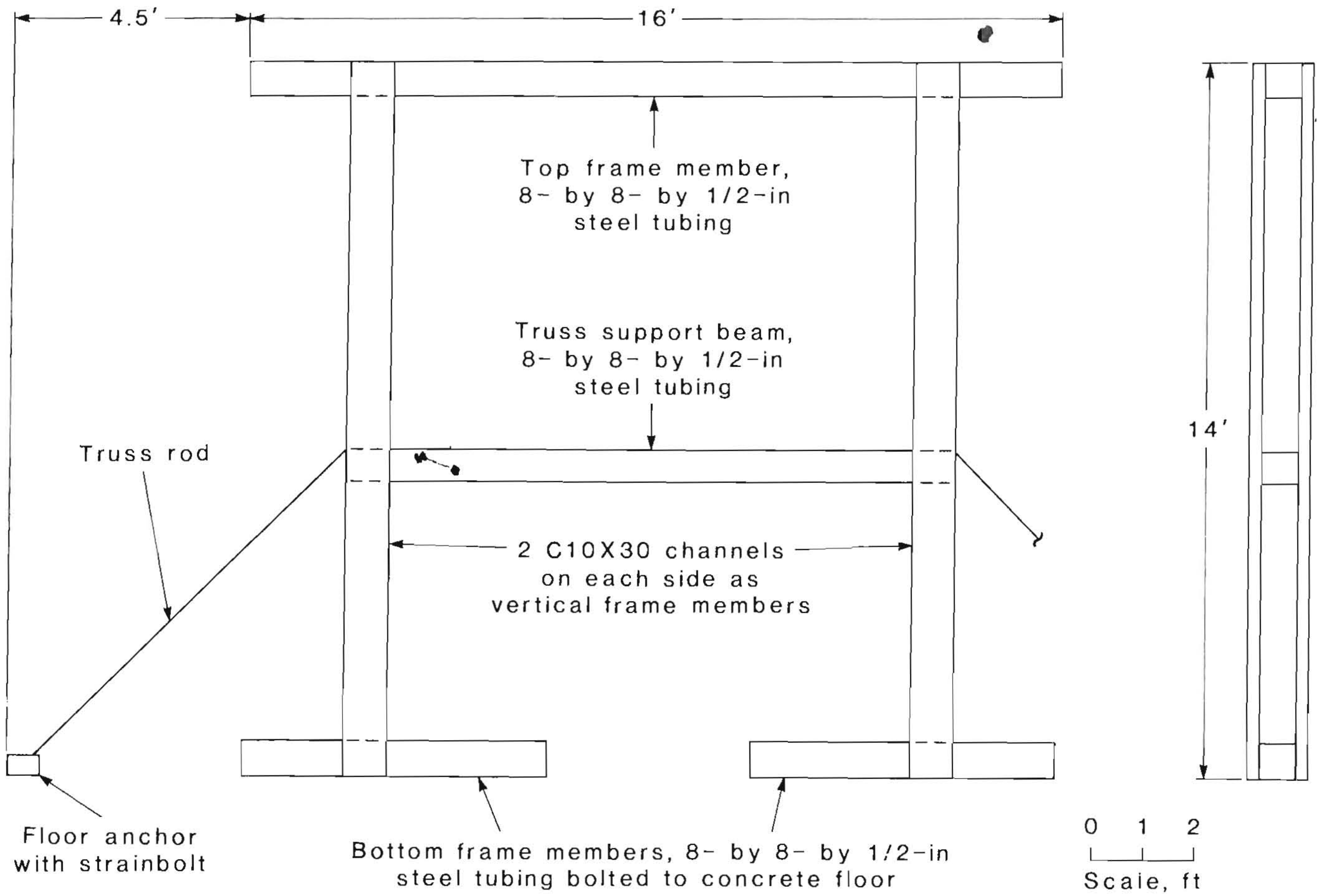

FIGURE 11.—Truss testing frame.

configuration. All gauges were covered with padding for protection.

Bearing Plate Load Cell

Figure 12 is a photograph of one of the two bearings plate load cells. These are 6 in wide, 4 in long, and 2 in high. A hardened, 2.0-in-radius, steel loading surface was machined to make contact with the truss rod. A rectangular hole was drilled in the load cell body on either side of the loading surface and strain gauges were mounted on both the front and back vertical surfaces. Both holes were then covered with thin plates for protection. The load cell body was mounted on two 0.5-in-diameter support rods to permit flexure under load. The load cells were designed and fabricated by a private company to measure forces in the vertical and horizontal directions. During a test, the cells were placed on top of the truss support beam at the required bearing plate positions.

Hole Collar Load Cell

A load cell was installed on each end of the truss support beam to simulate the contact point at the hole collar. These cells were made from a 9-in length of 2-in-diameter Acme screw. The top 4 in of the Acme thread was removed and the end was machined to a 1-in-radius curvature. The steel below the rounded end was machined to a rectangular cross section and strain gauges were mounted on the wider faces. The bottom of the cell was then screwed into mating threads in a steel block that was slipped into the end of the truss support beam. The top 4 in of the hole in the steel block was oversize so that the top of the load cell could flex under load without touching the sides of the hole. The cells were fabricated by a private company, and were designed to measure forces parallel and perpendicular to the cell axis. A view of the hole collar and bearing plate load cells supporting the truss rod is shown in figure 13.

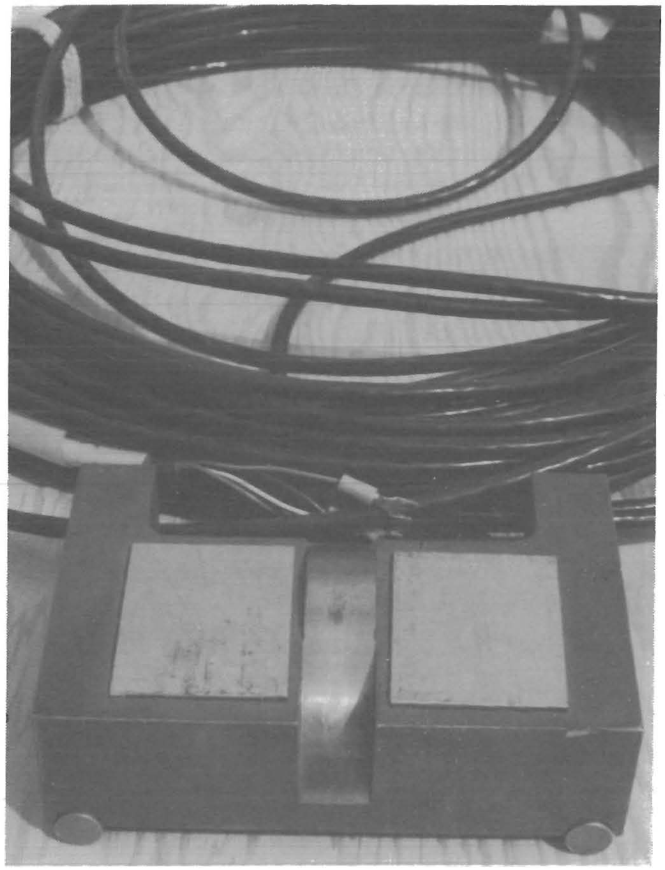

FIGURE 12.—Bearing plate load cell.

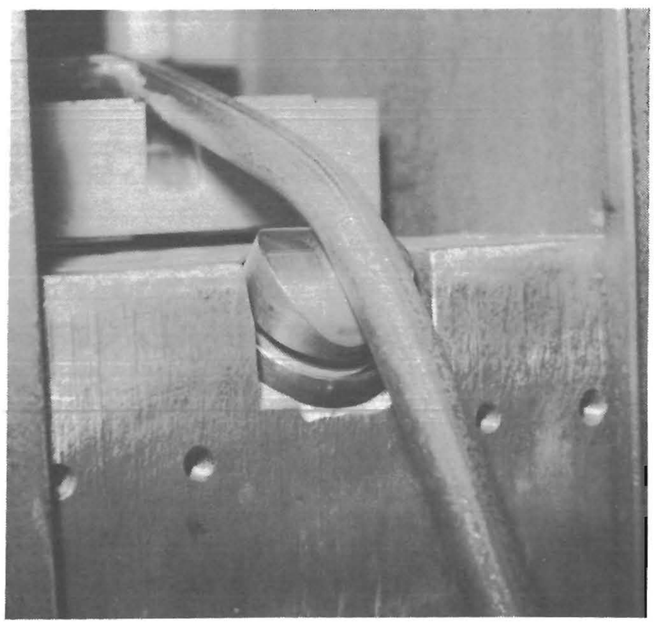

FIGURE 13.—Truss rod contacting bearing plate and hole collar load cells.

Floor Bolts

Three-fourths-inch-diameter Strainsert bolts were installed in the floor anchors to measure the tension in the inclined chord. They were inserted through a hole in the anchor stirrup and attached to the truss rod with a coupling. Figure 14 shows the truss rod connected to the floor bolt assembly. A view of the load cells and truss rod ready for a test is shown in figure 15.

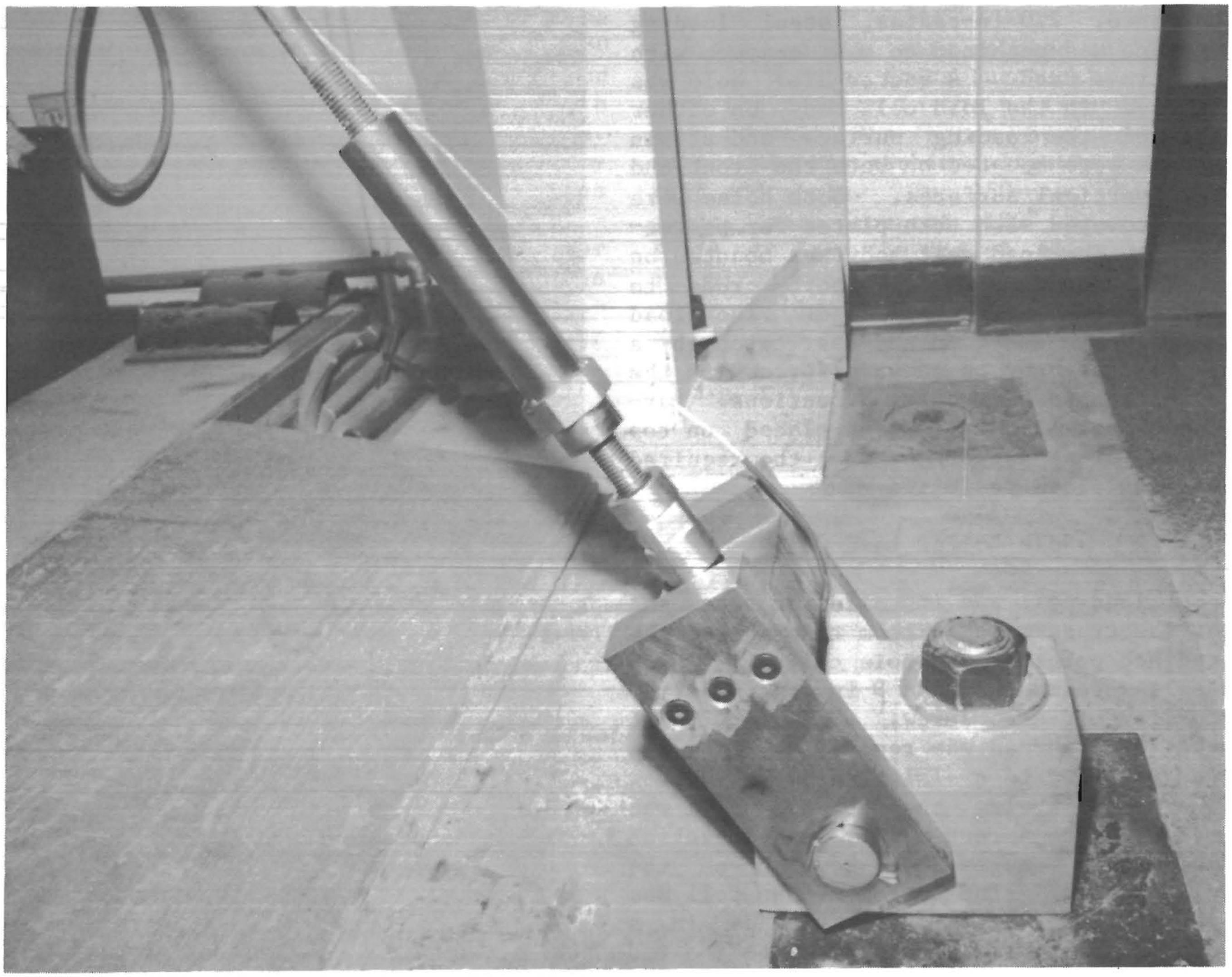

FIGURE 14.—Truss rod attached to floor bolt assembly.

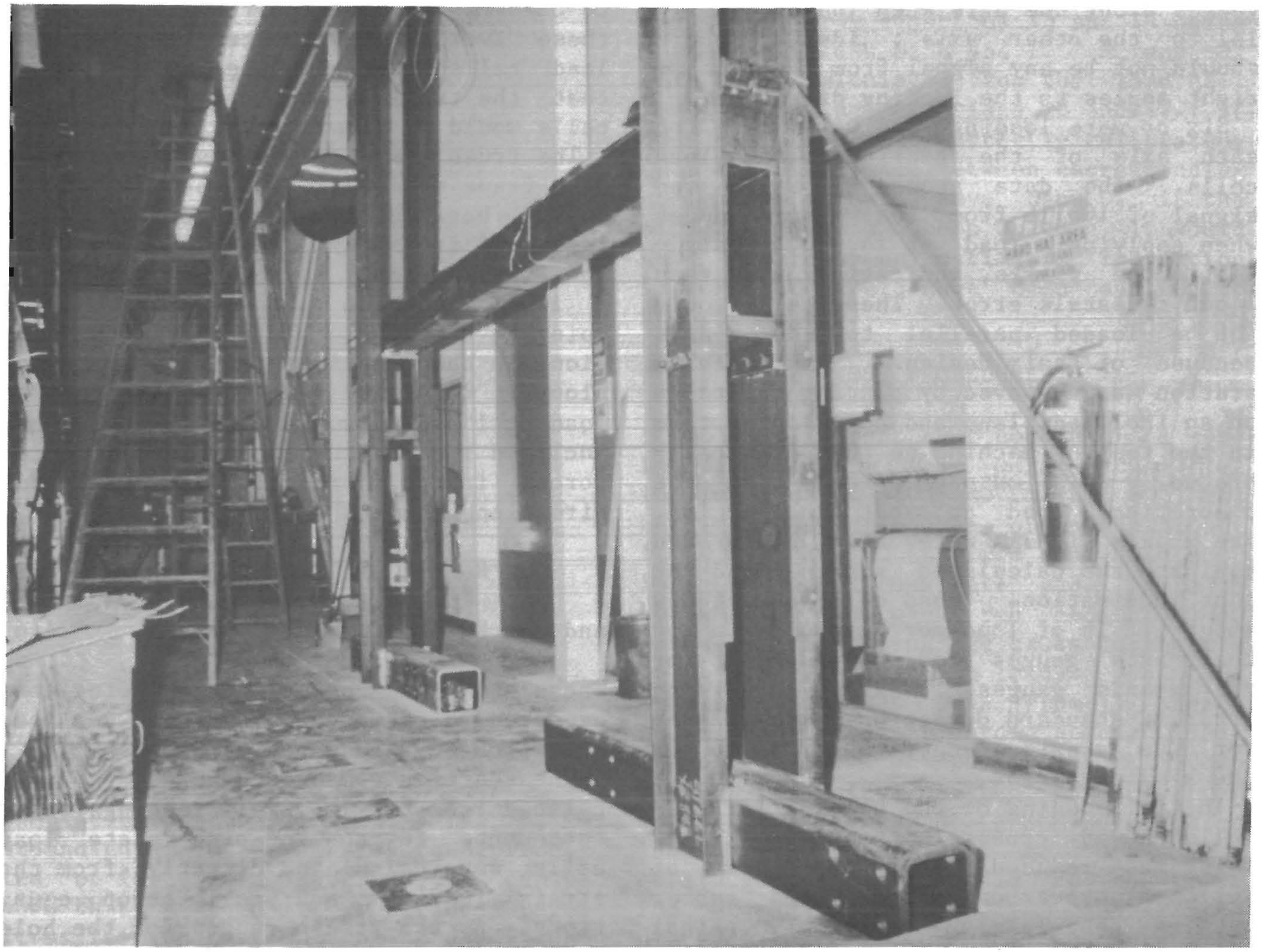

FIGURE 15.—Equipment assembled for testing.

EXPERIMENTAL PROCEDURE

LOAD CELL CALIBRATION

The load cells were calibrated on a Tinius Olsen testing machine and linear least squares calibration equations were fitted to the data. Crosstalk was expected to occur between the x- and y-axis gauges because they were bonded to the same piece of steel. Crosstalk is defined as "a false output signal from gauges along one axis when loading parallel to the other axis"; ideally, there should not be any signal from the axis at right angles to the loading direction.

Six or more loading runs were made for each axis of the bearing plate load cells. The data showed a false load signal of 100 lb from the x-axis gauges when applying a load of 14,000 lb parallel to the y-axis, indicating less than 1 pct crosstalk error. These cells could not be loaded parallel to the x-axis because of their design. X-axis calibration was achieved by placing the cells on an inclined plane and positioning them in the testing machine so that the calibrated y-axis output agreed with the theoretical load at that inclination. The x-axis signals were then calibrated against the calculated x-axis load at that inclination. Load cell output was about 12 lb of load per microstrain for the y-axis gauges and about 3.5 lb for the x-axis gauges. Maximum precision error (2 standard deviations) was ±124 lb for the y-axis gauges and ±268 lb for the x-axis gauges.

Initial loading of the hole collar load cells showed crosstalk of about 12 pct. This was reduced by using pieces of Teflon fluorocarbon polymer and rubber between the loading surfaces. Final results showed that an axial load of 20,000 lb produced a false transverse signal of about 120 lb, while a transverse load of 10,000 lb produced a false axial signal of about 400 lb. Six or more loading runs were made for each load cell axis and calibration equations were obtained for axial loading and for transverse loading in both positive and negative signal directions. Cell output was about 11 lb of load per microstrain for axial loading and 1.4 lb for transverse loading. Maximum precision error (2 standard deviations) was ±155 lb for the axial gauges and ±60 lb for the transverse gauges.

When conducting tests in the test frame, it was possible that the truss rods might have contacted the load cells at slightly different locations than that contacted by the testing machine head. Additional calibration runs were made with a truss installed in the test frame to check for possible differences between these two loading geometries. Only two load cells were calibrated at a time so that the tensions on both sides of the cells would be known.

The truss assembly was installed in the test frame and equal tensions were placed on the horizontal leg and both inclined legs. A free-body diagram for half of the truss assembly is shown in figure 16. H is the tension in the horizontal rod going to the turnbuckle and T is the tension in the inclined rod going to the floor. R is the reaction force at the load cell and a is the angle between the inclined rod and the floor. Summation of forces in the vertical and horizontal directions shows that:

$$R_v = T_y = T \sin a \tag{13}$$

and

$$R_h = H - T_x = H - T \cos a. \tag{14}$$

These equations permit calculating the expected reaction components at the load cell from the truss rod tensions.

The reaction components were also calculated from the load cell readings. The components for the bearing plate load cells were calculated directly from the strain readings and calibration equations. As the strain gauges for the hole collar load cells provided data in the axial and transverse directions, the vertical and horizontal components were calculated. The axial (A_a) and transverse (A_t) axes of the load cell are shown in figure 17, along with the reaction vector (R) and its vertical and horizontal components (R_v and R_h). A_a is inclined at 45° with the horizontal as this was the

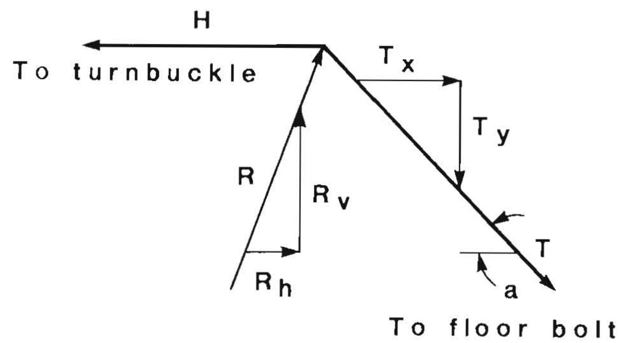

FIGURE 16.—Free-body diagram for test frame calibration.

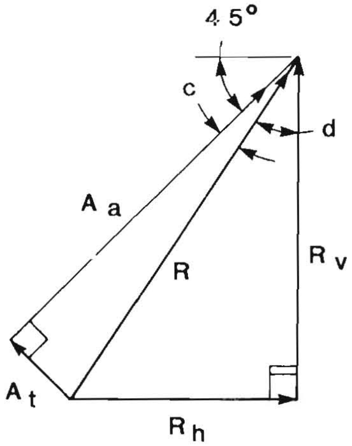

A_a is inclined at 45°

$d = 45° - c$

$\tan c = \frac{A_t}{A_a}$

$\sin d = \frac{R_h}{R}$

$\cos d = \frac{R_v}{R}$

FIGURE 17.--Force diagram for hole collar load cells.

orientation of the load cell axis. A_t is perpendicular to A_a. Using the principles of force parallelograms, it can be shown that R would be positioned below A_a, as its inclination from the horizontal was greater than 45° with equal tensions in the truss legs. The pertinent trigonometric relationships are listed on the figure. The axial and transverse forces on the load cell (A_a and A_t) were measured and the reaction components calculated as follows:

$$R = \sqrt{A_a^2 + A_t^2}, \qquad (15)$$

$$c = \tan^{-1} \frac{A_t}{A_a}, \qquad (16)$$

$$d = 45° - c, \qquad (17)$$

$$R_v = R \cos d, \qquad (18)$$

and

$$R_h = R \sin d, \qquad (19)$$

Expected values of R_v and R_h were calculated from equations 13 and 14 using measured values of H and T. R_v and R_h were also calculated from the load cell readings using equations 18 and 19. If the load cells were correctly calibrated, then the difference between corresponding components should have been 0. If the difference had not been 0, then it would have provided an estimated correction factor that could have been applied to the components.

TEST PROCEDURE

Twelve different test combinations were investigated. These were truss leg inclinations of 30°, 45°, and 60°, and bearing plate distances of approximately 6, 10, 20, and 40 in from the hole collar. Four test runs were made at each combination and each run consisted of manually tightening the truss turnbuckle to 6-, 11-, and 16-kip loads. (One kip equals 1,000 lb.) Data from 11 strain gauge channels was recorded at each load. These consisted of the turnbuckle, two Strainsert bolts, and two channels from each of the bearing plate and hole collar load cells. For some of the tests, strain gauges were bonded to the truss rod between the hole collar and bearing plate in order to directly measure P in this part of the rod.

A computer program was written to calculate all needed tensions and reaction components from the strain gauge data. In addition, estimates of P in the truss rod between the bearing plate and hole collar were calculated from the load cell data and equilibrium equations (see equations 5 and 7). Therefore,

$$P = \frac{BPV}{\sin b} \qquad (20)$$

and

$$P = \frac{T \sin a - HCV.}{\sin b} \qquad (21)$$

DATA ANALYSIS

The experimental T-H ratios obtained in the laboratory tests are listed in table 1. Each T-H ratio is the average of 12 numbers, i.e., the ratios for the four repetitive tests at 6, 11, and 16 kips were combined into one number. The angle from the end of the hole collar load cell to the top of the bearing plate (angle b) are those measured in the test frame; they differ slightly from the desired angles of a 2-in-high bearing plate at 6, 10, 20, and 40 in from the hole collar. A multiple regression analysis showed that the T-H ratios were independent of both a and b. The overall average of the listed T-H ratios was 0.881 with a 99-pct confidence interval of 0.858 to 0.905.

TABLE 1. - T-H ratios

Angle a, deg	Angle b, deg	Side of truss[1]	Average T-H ratio[2]
30	19.1	1	0.893
30	19.1	2	.908
30	10.8	1	.874
30	10.8	2	.889
30	5.1	1	.847
30	5.1	2	.857
30	2.7	1	.853
30	2.7	2	.846
45	19.1	1	.963
45	19.1	2	.940
45	10.8	1	.948
45	10.8	2	.926
45	5.1	1	.892
45	5.1	2	.881
45	2.7	1	.874
45	2.7	2	.834
60	19.1	1	.833
60	19.1	2	.787
60	10.8	1	.854
60	10.8	2	.845
60	5.1	1	.903
60	5.1	2	.886
60	2.7	1	.920
60	2.7	2	.904

[1]1 and 2 indicate the two sides of the same truss.

[2]Each T-H ratio is the average of 12 tests.

The experimental P-H ratios obtained in the laboratory tests are listed in table 2. Each P-H ratio is the average of 12 numbers, similar to the T-H ratios. Three estimates of P were made. P was calculated from the equilibrium equations and load cell data using equations 20 and 21. In some of the tests, data obtained from the strain gauges attached to the truss rod were also used to calculate P. The source of the P estimate is denoted in column 4, "Source of P."

The accuracy of the load cells is questionable, as column 5 contains several experimental P-H ratios greater than 1. P should be less than H and the P-H ratio should be less than 1. Also, during some of the laboratory tests, negative transverse signals were recorded from the hole collar load cells, indicating that frictional drag from the truss rod might be bending the load cell sideways. An indication of load cell accuracy can be obtained by plotting BPV-H versus sin b and observing if the experimental P-H ratio agrees with the theoretical curves of figure 3. For example, consider the data on the fifth line of table 2, i.e., b = 10.8, sin b = 0.187, P-H = 0.96, and BPV-H = 0.18. The resulting point would plot slightly above the curve for P = 0.95 H in figure 3, indicating a theoretical P-H value of about 0.96 which is the same as the value in the table. Values of BPV-H are listed in column 6; they were obtained by dividing the vertical reaction component at the bearing plate, as calculated from the load cell data, by H. In order to obtain a numerical estimate of accuracy, the numbers in the theoretical P-H column (column 7) were calculated from the equilibrium equations using experimental values of BPV-H and sin b, that is,

$$\text{P-H} = (\text{BPV-H})/\sin b. \qquad (22)$$

A maximum value of 1 was listed in the table when the theoretical P-H ratio was greater than 1, as P should not be greater than H.

TABLE 2. - P-H ratios

Angle a, deg	Angle b, deg	Side of truss[1]	Source of P[2]	Experimental P-H ratio[3]	BPV-H ratio	Theoretical P-H ratio	Difference, pct	Acceptable P-H ratios
30	19.1	1	BP	1.098	0.359	1.0	9.8	
30	19.1	1	HC	1.149	.359	1.0	14.9	
30	19.1	2	BP	1.053	.344	1.0	5.3	
30	19.1	2	HC	1.149	.344	1.0	14.9	
30	10.8	1	BP	.960	.180	.961	-.1	0.960
30	10.8	1	HC	.962	.180	.961	.1	.962
30	10.8	1	SG	.952	.180	.961	-.9	.952
30	10.8	2	BP	.923	.173	.923	.0	.923
30	10.8	2	HC	.923	.173	.923	.0	.923
30	10.8	2	SG	.916	.173	.923	-.8	.916
30	5.1	1	BP	.962	.086	.967	-.5	.962
30	5.1	1	HC	.940	.086	.967	-2.8	.940
30	5.1	1	SG	.972	.086	.967	.5	.972
30	5.1	2	BP	.948	.084	.945	.3	.948
30	5.1	2	HC	.907	.084	.945	-4.0	.907
30	5.1	2	SG	.982	.084	.945	3.9	.982
30	2.7	1	BP	.875	.041	.870	.6	.875
30	2.7	1	HC	.689	.041	.870	-20.8	
30	2.7	1	SG	.969	.041	.870	11.4	
30	2.7	2	BP	.863	.041	.870	-.8	.863
30	2.7	2	HC	.808	.041	.870	-7.1	
30	2.7	2	SG	.973	.041	.870	11.8	
45	19.1	1	BP	.893	.292	.892	.1	.893
45	19.1	1	HC	.984	.292	.892	10.4	
45	19.1	2	BP	.898	.294	.898	.0	.898
45	19.1	2	HC	.995	.294	.898	10.8	
45	10.8	1	BP	.912	.171	.913	-.1	.912
45	10.8	1	HC	1.031	.171	.913	12.9	
45	10.8	2	BP	.917	.172	.918	-.1	.917
45	10.8	2	HC	.976	.172	.918	6.3	
45	5.1	1	BP	.925	.082	.922	.4	.925
45	5.1	1	HC	1.027	.082	.922	11.4	
45	5.1	2	BP	.946	.084	.945	.2	.946
45	5.1	2	HC	.964	.084	.945	2.0	.964
45	2.7	1	BP	.858	.040	.849	1.1	.858
45	2.7	1	HC	.997	.040	.849	17.4	
45	2.7	2	BP	.876	.041	.870	.7	.876
45	2.7	2	HC	.826	.041	.870	-5.1	

See footnotes at end of table.

TABLE 2. - P-H ratios--Continued

Angle a, deg	Angle b, deg	Side of truss[1]	Source of P[2]	Experimental P-H ratio[3]	BPV-H ratio	Theoretical P-H ratio	Difference, pct	Acceptable P-H ratios
60	19.1	1	BP	1.144	0.374	1.0	14.4	
60	19.1	1	HC	.784	.374	1.0	-21.6	
60	19.1	2	BP	1.114	.365	1.0	11.4	
60	19.1	2	HC	.719	.365	1.0	-28.1	
60	10.8	1	BP	1.069	.200	1.0	6.9	
60	10.8	1	HC	1.072	.200	1.0	7.2	
60	10.8	1	SG	1.056	.200	1.0	5.6	
60	10.8	2	BP	1.104	.207	1.0	10.4	
60	10.8	2	HC	1.040	.207	1.0	4.0	1.040
60	10.8	2	SG	1.013	.207	1.0	1.3	1.013
60	5.1	1	BP	1.044	.093	1.0	4.4	1.044
60	5.1	1	HC	.974	.093	1.0	-2.6	.974
60	5.1	1	SG	1.061	.093	1.0	6.1	
60	5.1	2	BP	1.093	.097	1.0	9.3	
60	5.1	2	HC	1.038	.097	1.0	3.8	1.038
60	5.1	2	SG	1.042	.097	1.0	4.2	1.042
60	2.7	1	BP	.848	.040	.849	-.1	.848
60	2.7	1	HC	.735	.040	.849	-13.4	
60	2.7	1	SG	1.048	.040	.849	23.4	
60	2.7	2	BP	.906	.043	.913	-.8	.906
60	2.7	2	HC	.938	.043	.913	2.7	.938
60	2.7	2	SG	1.008	.043	.913	10.4	

[1]1 and 2 indicate the two sides of the same truss.

[2]BP indicates that P was calculated from the bearing plate load cell data; and HC indicates that P was calculated from the hole collar load cell data; and SG indicates that P was calculated from strain gauges bonded to the truss rod.

[3]Each P-H ratio is the average of 12 tests.

The percentage difference between the experimental and theoretical P-H values is listed in column 8. These differences ranged from 0 to 28 pct. The acceptable P-H ratios, where the difference was less than 5 pct, are listed in the last column of the table. A multiple regression analysis showed that the P-H ratios were independent of both a and b. The overall average of the acceptable P-H ratios was 0.941 with a 99-pct confidence interval of 0.915 to 0.967.

UNDERGROUND TESTS[7]

Over a period of 3 yr, beginning in June of 1978, Mangelsdorf monitored the underground installation of a number of Birmingham trusses in three mines. Although the primary purpose of his study was the determination of the relation between tension and frequency of vibration in the horizontal chords,[8] he also recorded tensions in the inclined chords with strain gauges. All the inclined

[7]Data furnished by C. P. Mangelsdorf, Univ. of Pittsburgh, Pittsburgh, PA.

[8]Mangelsdorf, C. P. Evaluation of Roof Trusses, Phase II. Use of Frequency of Vibration to Determine Chord Tension (contract 50100070, Univ. Pittsburgh). BuMines OFR 35-84, 1983, 58 PP.; NTIS PB 84-166479.

chords were nominally at 45°, but no effort was made to control the angle strictly.

Mine 1 was located in western Kentucky, mine 2 was located in southern Illinois, and mine 3 was located in southern West Virginia. Mines 1 and 2 had roofs of shale while mine 3 had a sandstone roof. Both new and previously installed truss rods were used. Installation tensions ranged from 9,410 to 14,587 lb.

It should be noted that T-H values changed very rapidly at installation due to crushing of the roof and "settling in" of the truss components. While both T and H decreased, H decreased more rapidly, thus tending to increase the T-H values. As no effort was made to standardize the tightening procedure beyond that normally used by the truss crew, and because the recording sequences of the various chords were not consistent, it seems likely that the scatter of the data was the result of the rapidly changing tension.

The underground T-H ratios are listed in table 3. A statistical analysis showed no significant difference between the T-H ratios for the new and used truss rods in mine 2. Also, no significant difference was found between the T-H ratios for the shale roof in mine 2 and the sandstone roof in mine 3. Consequently, all T-H ratios were combined into one group. Their average value was 0.908 with a 99-pct confidence interval of 0.873 to 0.943.

TABLE 3. - T-H ratios for underground tests

Truss condition	Side of truss[1]	H, lb	T-H ratio
MINE NO. 1			
Used	1	9,997	1.077
Do	2	9,997	1.079
Do	1	9.731	1.037
Do	2	9,731	.947
Do	1	9,767	.918
Do	2	9,767	1.002
Do	1	9,813	.908
Do	2	9,813	.982
Do	1	9,410	1.019
Do	2	9,410	.876
Do	1	10,080	.916
Do	2	10,080	.968
MINE NO. 2			
New	1	11,346	0.96
Do	2	11,346	.82
Do	1	12,640	.84
Do	2	12,640	.87
Do	1	14,587	.83
Do	2	14,587	.92
Do	1	13,045	.80
Do	2	13,045	.88
Do	1	11,107	1.09
Do	2	11,107	1.02
MINE NO. 2--Con.			
Used	1	10,550	0.91
Do	2	10,550	.91
Do	1	10,150	.99
Do	2	10,150	.84
Do	1	12,700	.79
Do	2	12,700	.86
Do	1	10,560	.84
Do	2	10,560	.85
Do	1	10,590	.88
Do	2	10,590	.96
MINE NO. 3			
New	1	11,466	0.87
Do	2	11,466	.97
Do	1	11,126	.81
Do	2	11,126	.89
Do	1	11,227	.79
Do	2	11,227	.83
Do	1	11,163	.74
Do	2	11,163	.79
Do	1	10,796	.98
Do	2	10,796	.88

[1] 1 and 2 indicate the two sides of the same truss.

NOTE.--Angle a is approximately 45° for all cases.

TYPICAL TRUSS FORCES

Typical loads that a truss would apply to roof strata can be calculated from the equilibrium equations. T-H ratios of 0.881 and 0.908 were obtained from laboratory and underground tests, respectively. Consequently, it seems reasonable to expect a T-H ratio of about 0.90 for underground truss installations. Assuming the inclined legs at 45° and substituting P-H = 0.94 and T-H = 0.90 in the equilibrium equations, with H = 10,000 lb and the bearing plate 10 in from the hole collar, then:

$$P = 9{,}400 \text{ lb},$$

$$T = 9{,}000 \text{ lb},$$

$$b = \text{arc tan } (2/10) = 11.3099°,$$

$$BPV = P \sin b = 9{,}400 \sin (11.3099)$$

$$= 1{,}843 \text{ lb},$$

$$BPH = H - P \cos b$$

$$= 10{,}000 - 9{,}400 \cos (11.3099)$$

$$= 783 \text{ lb},$$

$$HCV = T \sin a - P \sin b$$

$$= 9{,}000 \sin (45) - 9{,}400 \sin (11.3099)$$

$$= 4{,}520 \text{ lb},$$

and

$$HCH = P \cos b - T \cos a$$

$$= 9{,}400 \cos (11.3099) - 9{,}000 \cos (45)$$

$$= 2{,}853 \text{ lb}.$$

Because forces that the truss applies to the roof strata instead of the reaction in the rock are being considered, the arrow directions would be reversed from those shown in figure 2. A positive BPV or HCV is directed upwards, while a positive BPH or HCH is directed to the right or towards the centerline of the entry. At the bearing plate, the truss would push against the roof with a vertical force of 1,843 lb directed upwards and a horizontal force of 783 lb directed toward the center of the entry. At the hole collar, the truss would push against the roof with a vertical force of 4,520 lb directed upwards and a horizontal force of 2,853 lb directed toward the center of the entry. These forces are illustrated in figure 18.

FINITE-ELEMENT ANALYSIS

The effect of truss loads on stresses in roof strata was investigated using a linear finite-element analysis. A 20-ft-wide entry located 1,000 ft below the surface was modeled with horizontal stresses equal to the vertical stresses. Twelve-foot-long trusses on four-foot centers with 45° inclined legs were used. The bearings plate was located 10 in from the hole collar. The loads that would be produced by this truss configuration tensioned to 10,000 lb were placed on the roof strata. Stresses due to gravity loading only were analyzed first. Horizontal compressive stresses up to 3,000 psi and vertical compressive stresses up to 1,500 psi were obtained. The forces applied by the tensioned truss were then added to the model, which produced a negligible change in the stress field. As a check, the analysis was rerun with only the truss loads applied to the model. The maximum stress induced

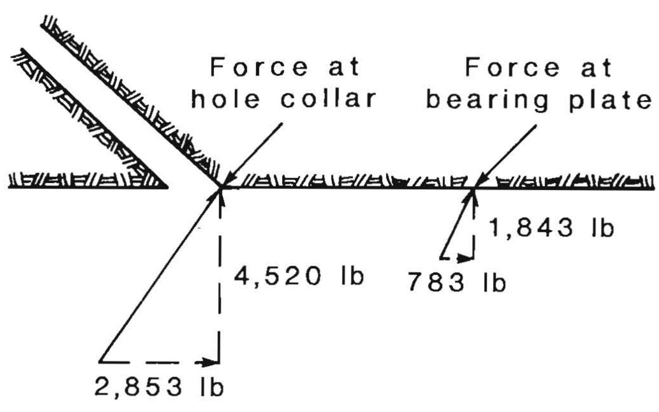

FIGURE 18.—Typical roof forces generated by a tensioned truss.

by the truss loads in the roof strata was only 8 psi.

This indicates that trusses would probably have little effect when installed in roofs composed of competent, continuous rock. However, many roofs are composed of layered, broken strata, and trusses would probably be more effective in such roofs. This situation cannot be adequately modeled by finite-element methods at the present time.

CONCLUSIONS

Theoretical reaction forces between the truss and the roof strata can be calculated from the installation geometry and assumed values for the P-H and T-H ratios.

Actual reaction forces for an individual truss are difficult to estimate as the P-H and T-H ratios can vary widely because of the variable friction losses at the contact points.

P-H and T-H ratios of 0.94 and 0.90 are recommended for calculating reaction forces.

APPENDIX.--EXPLANATION OF SYMBOLS

a	Angle between inclined chord of the truss and the horizontal.
A_a	Axial force on the hole collar load cell.
A_t	Transverse force on the hole collar load cell.
b	Angle between the segment of truss rod between the hole collar and bearing plate and the horizontal.
BPH	Horizontal component of the bearing plate reaction force.
BPV	Vertical component of the bearing plate reaction force.
c	Angle between the hole collar load cell axis and inclination of the reaction force, used when calibrating load cells in the test frame.
d	Angle between the reaction force inclination and the vertical, used when calibrating load cells in the test frame.
H	Tension in the horizontal chord of the truss.
HCH	Horizontal component of the hole collar reaction force.
HCV	Vertical component of the hole collar reaction force.
P	Tension in the truss rod segment between the hole collar and bearing plate.
P_x	Horizontal component of P.
P_y	Vertical component of P.
R	Load cell reaction force, used when calibrating load cells in the test frame.
R_h	Horizontal component of R.
R_v	Vertical component of R.
T	Tension in the inclined chord of the truss.
T_x	Horizontal component of T.
T_y	Vertical component of T.

U.S. GOVERNMENT PRINTING OFFICE: 1988 — 547-000/80,026

INT.-BU.OF MINES,PGH.,PA. 28674